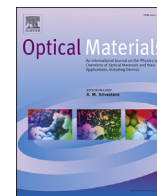




Contents lists available at ScienceDirect

Optical Materials

journal homepage: www.elsevier.com/locate/optmat

Compaction and flow rule of oxide nanopowders

G. Sh. Boltachev^{a,*}, K.E. Lukyashin^a, A.L. Maximenko^b, R.N. Maksimov^{a,c}, V.A. Shitov^a, M.B. Shtern^b^a Institute of Electrophysics, Ural Branch of RAS, Amundsen St. 106, Ekaterinburg 620016, Russia^b Frantsevich Institute for Problems of Materials Science, NAS Ukraine, Krzhizhanovsky St. 3, Kyiv 03680, Ukraine^c Ural Federal University Named After the First President of Russia B.N. Yeltsin, Mira St. 19, Ekaterinburg 620002, Russia

ARTICLE INFO

Article history:

Received 10 February 2016

Received in revised form

25 September 2016

Accepted 25 September 2016

Available online xxx

Keywords:

Oxide nanopowder

Cold compaction

Yield surface

Flow rule

ABSTRACT

Transparent Al₂O₃ ceramics have attracted considerable interest for use in a wide range of optical, electronic and structural applications. The fabrication of these ceramics using powder metallurgy processes requires the development of theoretical approaches to the compaction of nanopowders. In this work, we investigate the compaction processes of two model granular systems imitating Al₂O₃ nanosized powders. System I is a loosely aggregated powder, and system II is a powder strongly inclined to agglomeration (for instance, calcined powder). The processes of isostatical (uniform), biaxial, and uniaxial compaction as well as uniaxial compaction with simultaneous shear deformation are studied. The energy parameters of compaction such as the energy change of elastic interparticle interactions and dispersion interactions, dissipative energy losses related to the processes of interparticle friction, and the total work of compaction are calculated for all the processes. The nonapplicability of the associated flow rule to the description of deformation processes of oxide nanopowders is shown and an alternative plastic flow rule is suggested. A complete system of determining the relationship of the flow including analytical approximations of yield surfaces is obtained.

© 2016 Elsevier B.V. All rights reserved.

1. Introduction

In recent years, polycrystalline ceramic materials based on refractory oxides such as Al₂O₃ [1–8] and Y₂O₃ [7,9,10] have enjoyed considerable research interest as potential candidates for various optical applications. In particular, high heat conductivity is a known advantage of aluminium oxide as a laser medium [6]. The average grain size and the sizes of residual pores must be decreased by up to the values of about 10 nm in order to achieve high optical quality and a desirable mechanical resistance of alumina ceramics [2,6]. Hence, the development of nanotechnologies and, in particular, the fabrication of nanostructured ceramics using powder metallurgy processes is closely connected with a growing interest in transparent ceramics [4,6–10]. The cold compaction of nanosized powders is the most commonly used processing step for powder metallurgy [7–11]. In contrast to micron (or larger) powders, nanopowders possess a number of unexpected properties [11–13], which have an influence on powder compaction and subsequent

sintering. Primarily, they have a pronounced size-related effect: the smaller the particle size, the harder it is to compact the powder [12,13]. In some cases the pressure of several GPa is required to obtain a desired density of oxide nanopowder during the cold compaction process [9,11–13]. In addition, as demonstrated in Refs. [12,13], the nanopowders of oxide materials are beyond the associated flow rule and are weakly sensitive to the compaction method since the difference in the density after isostatical (uniform) and uniaxial pressing does not exceed 1%.

The rapid development of experimental methods and further success in the fabrication of nanostructured oxide ceramics require the corresponding development of theoretical conceptions of the mechanical properties of the nanopowder compact. In the space of stress tensor invariants the yield surface has a convex form of an elliptical type [12,13] that is supposed to rely on the theory of plastically hardening porous bodies as a continuum approach for describing the properties of the nanopowder [11,14]. Thus, obviously, a number of conceptions and a terminology related to the theory attain a conditional character, in particular, that the plasticity of a powder body is correlated with the processes of the mutual sliding and rearrangement rather than the deformation of the individual particles. The features of the nanopowder body

* Corresponding author.

E-mail address: grey@iep.uran.ru (G.Sh. Boltachev).

demand a serious inspection of the main conceptions of the theory and verification of its results towards the properties of the described body. A full-scale experiment is unable to give comprehensive information on the characteristics of the powder system and the evolution of its properties during the compaction processes. In fact, from the experiment we only find the powder compaction curve under well-defined pressing conditions.

Far more detailed information can be obtained within the framework of the microscopic investigation presented in this paper, i.e. a computer simulation of the powder by the granular dynamics method [12,13]. For research objects, we use two monosized model systems (the particle diameter $d = 10$ nm) corresponding to alumina nanopowders, which have a weak (system I) and strong (system II) inclination to agglomeration [12]. Such powders are produced by the Institute of Electrophysics (Ekaterinburg, Russia) by electric explosion of wires [15] and by laser ablation [9,16]. The individual particles have a spherical form and high strength properties. The particle sphericity, high strength, and nonsusceptibility to plastic deformation make granular dynamics a promising and adequate tool of theoretical analysis.

2. Calculation

In this study, the processes of cold quasistatic pressing such as isostatical compaction (process A), biaxial (B) and uniaxial (C) compaction, and uniaxial compaction with simultaneous shear deformation (D) are simulated by the granular dynamics method in 3D geometry. These processes are performed by simultaneous changes of selected sizes of a model cell (all sizes when simulating the process A; the cell height z_{cell} when simulating the uniaxial compaction; and so on) and proportional rescaling of the appropriate coordinates of all the particles. After each step of deformation, the new equilibrium locations of the particles are determined during a large number N_{iter} of equilibration steps (several hundred, as a rule). This work is a continuation and development of studies presented in Refs. [12,13], in which the above-mentioned processes and all the interparticle interactions used in the model are described in detail. Here we point out that the interactions of particles include elastic repulsion, tangential “friction” forces, resistance to relative rotation of particles and their “rolling”, dispersion forces of attraction, and the possible formation of strong bonds of a chemical nature for system II. The parameters of particles material correspond to α phase of aluminium oxide. Examples of this are Young's modulus $E = 382$ GPa, Poisson's ratio $\nu = 0.25$, and the dispersive energy of intermolecular attraction $\varepsilon = 1224 k_B$ (k_B is the Boltzmann's constant). The number of particles in a model cells $N_p = 1000$, and the maximum compaction pressure $p_{max} = 5$ GPa. Such high pressure is not achievable using the experimental equipment for static compaction, but could be obtained by inertial effects during the processes of magnetic pulsed compaction [11].

In contrast to earlier studies [12,13], in this work we have added minor changes to the numerical algorithm in order to increase accuracy during the calculation of the compaction curves. The number of independent computer experiments for statistical averaging when plotting the calculated curves was increased by four times (from 10 to 40); the maximum number of equilibration steps $N_{iter,max}$ for achieving new equilibrium locations of the particles was increased by two times (up to 2000); and the minimum value of the particle attractive force $f_{a,min}$ (where the cutting of the dispersive potential occurred) was decreased from 5×10^{-6} to 1×10^{-6} (in reduced units: $f_{red} = f/(Ed^2)$). These minor modifications of the numerical algorithm led to small shifts in the compaction curves presented in Ref. [13]. The shifts are not visually recognizable (the density shifts are about 0.2%), but they have

sufficient amplitude in the pressures (about 100 MPa at the maximum compaction pressures). As a result, this led to a significant change in the yield surfaces of the investigated systems (Fig. 1) corresponding to the defined values of compact unloading density ρ_u , i.e., the density of compact after the removal of the external load. Primarily, this is related to System II (with strong bonds). In particular, process D now has higher values of the deviator intensity τ compared with process C throughout the whole range of investigated loads up to pressures of $p_{max} = 5$ GPa. It was previously observed only in a loading range below 3 GPa [13]. Note that the process of pure shear E as shown in Fig. 1 was not calculated in this work and the corresponding points were taken from Ref. [13]. The analysis performed makes it clear that the primary factor resulting in the change of yield surfaces is the increase of the $N_{iter,max}$ parameter. This fact indicates that the yield surface is a very sensitive property of the simulated systems and a reliable calculation of the yield surface requires a high level of accuracy in the achievement of an equilibrium state for all the particles after every deformation step of a model cell.

3. Results and discussion

3.1. Energy parameters of the compaction processes

Despite the change of the yield surfaces noted in Sec. 2, one of the main conclusions of Ref. [13], i.e. nonapplicability of the associated flow rule to the oxide nanopowders, remains valid. To find another flow rule of the compacted medium, which could be used instead of the associated rule, energy parameters such as the energy of the particles' elastic strains E_{el} , the energy of dispersive attractions E_a , and dissipative energy losses related to the processes of interparticle friction W_f were investigated in this study. Fig. 2 shows the total work of powder compaction $W_{out} = \Delta E_{el} + \Delta E_a + W_f$ and its part coming from dissipative losses to the interparticle friction W_f . As can be seen, up to densities of about 60% the compression work is mainly expended to overcome the interparticle friction. Here the significant rearrangement of particles occurs, the average coordination number increases notably, and the effective compaction of a powder body is performed. A further increase in pressure leads to a considerable growth of the elastic stresses, i.e. a powder structure is “stuck” in a fixed configuration. Subsequent deformation of a model cell (at $\rho > 0.6$) becomes more and more elasto-reversible, and the unloading density of the compact ρ_u practically stops increasing. In addition, Fig. 2 shows that the values of W_{out} and W_f significantly depend on the process being performed. This indicates that the powder could not be characterized by a universal relationship $W(\rho)$ or $W(\rho_u)$ and, as a consequence, it is impossible to expect a coincidence in the space of stress tensor invariants with the yield surfaces satisfying the $\rho_u = \text{const}$ condition and the levels of the plastic potential ($W_f = \text{const}$) determining the energy dissipation rate.

Fig. 3 presents the levels corresponding to the fixed values of the total strain W_{out} and the dissipative losses W_f . On a plane (p, τ), where p is the hydrostatic pressure and τ is the deviator intensity of the stress tensor, these levels are well-approximated by the following equation:

$$\tau(p) = (c_1 + c_2 p) \sqrt{(1 - \alpha)^2 p_A^2 - (p - \alpha p_A)^2}, \quad (1)$$

where the hydrostatic pressure at the isostatic compaction p_A is used as a parameter characterizing the fixed level, parameter $c_2 > 0$ for levels of W_{out} and $c_2 = 0$ for levels of W_f . An analytical description of W_{out} and W_f levels by Eq. (1) simplifies their theoretical analysis. To the left of the maximum (where $\partial W_{out}/\partial p = 0$, or

Download English Version:

<https://daneshyari.com/en/article/5442561>

Download Persian Version:

<https://daneshyari.com/article/5442561>

[Daneshyari.com](https://daneshyari.com)